POTENTIAL OF BUILDING EXTRACTION FROM MULTI-ASPECT HIGH-RESOLUTION AMPLITUDE SAR DATA

E. Michaelsen, U. Soergel, U. Thoennessen

FGAN-FOM Research Institute for Optronics and Pattern Recognition, Gutleuthausstraße 1, 76275 Ettlingen, Germany

mich@fom.fgan.de

KEY WORDS: SAR, Building, Detection, Reconstruction, Urban, GIS, Fusion

ABSTRACT:

State-of-the-art airborne SAR sensors provide spatial resolution on the order of a decimetre. In such data, many features of urban objects can be identified, which were beyond the scope of radar remote sensing before. In this paper, the impact of high-resolution SAR data on the analysis of urban scenes is discussed. The new quality of the appearance of buildings in such data is discussed with a couple of SAR images taken from orthogonal viewing directions. The topics geocoding and data fusion using different kinds of reference GIS data are addressed. The fine level of detail opens the opportunity to reconstruct the structure of man-made objects (e.g. buildings). A concept for the radargrammetric building analysis from high-resolution amplitude SAR imagery is proposed and preliminary results are presented.

1. INTRODUCTION

In general, topographic mapping of urban areas is based on sensor data acquired from airborne platforms in nadir view under good weather conditions, e.g. aerial imagery and LIDAR. An alternative part of the frequency spectrum of steadily growing importance in remote sensing is the radar domain. Synthetic aperture radar (SAR) sensors provide a two-dimensional mapping of the scene. However, the SAR principle requires an oblique and side-looking viewing direction [Schreier, 1993]. Consequently, occlusions and multi-bounce signal propagation occur frequently in urban areas [Dong et al., 1997]. Additionally, layover inevitably takes place at building locations. These effects burden radargrammetic approaches for the analysis of urban scenes [Leberl, 1990] (e.g. SAR stereoscopy), due to the strong dissimilarity of images (resulting in a lack of suitable tie points) even in the case of only small changes of the illumination aspect. For this reason radargrammetric stereo has recently been approached on datasets with parallel trajectory and viewing direction but differing in depression angle [Simonetto et al., 2003]. SAR has some very significant advantages compared to complementary sensors like aerial photography: because of the active scene illumination, SAR is independent of the daytime and the large signal wavelength provides almost insensitivity to weather conditions. These features suggest utilizing SAR for event-driven mapping tasks [Soergel et al., 2003a], which may be requested for traffic monitoring [Stilla et al., 2004], disaster management [Kakumoto et al., 1997], and damage assessment [Shinozuka et al., 2000] in case of a flooding or an earthquake [Takeuchi et al., 2000].

Commercial airborne SAR sensors typically provide data of spatial resolution on the order of a meter and currently developed space-borne systems will achieve similar values [Roth, 2003]. First results of experimental airborne SAR systems have shown that objects of size even below a decimetre can be resolved [Brenner and Ender, 2002]. In such data many features of urban objects can be identified, which were beyond the scope of radar remote sensing before. This seems to offer the opportunity to overcome some limitations of building recognition from SAR data in dense urban areas [Gamba et al, 2000; Soergel et al., 2003b].

In this paper, the impact of high-resolution SAR data on the analysis of urban scenes is described in the context of a retrieval of geometric features of objects. Examples for the new quality of the appearance of buildings in data of decimetre resolution are given and interpreted in Section 2, using two SAR images taken from orthogonal viewing directions.

The topics geocoding and data fusion are addressed in Section 3. The fusion aspect is vital for a reliable analysis of high-resolution SAR data of urban scenes, because the interpretation of such data is a demanding task even for experts [Soergel et al., 2004]. The pros and cons of different types of symbolic reference data, e.g. 2D maps and 3D city models (prismatic and polyhedral building representation), are discussed.

The signal of roof structures such as eaves and ridges or facade elements appear for the first time well contrasted in the SAR imagery. Such features can now be used as tie structures for a radargrammetric analysis of the building geometry. An approach based on concepts of SAR stereoscopy is proposed in Section 4 and first results are given. The recognition is carried out using a production system [Stilla et al., 1996].

2. BUILDING STRUCTURES IN HIGH-RESOLUTION SAR DATA

The appearance of buildings in high-resolution SAR images is discussed using a subset of the test area Karlsruhe University campus (Germany). Fig 1a depicts an InSAR magnitude image of about one meter resolution (range: top-down), which was acquired by the AER-II sensor of FGAN in 1998 [Ender, 1998]. The very same part of the scene was mapped again in summer 2002 twice from the same and an orthogonal aspect, this time with the new FGAN sensor PAMIR [Ender and Brenner, 2003]. The resolution of the sliding-mode multilook amplitude image presented in Fig 1b is slightly better than 20cm in range and azimuth (HH polarization, off-nadir angle 55°). The X-band sensor is capable to provide even better resolution, below one decimetre in both directions.
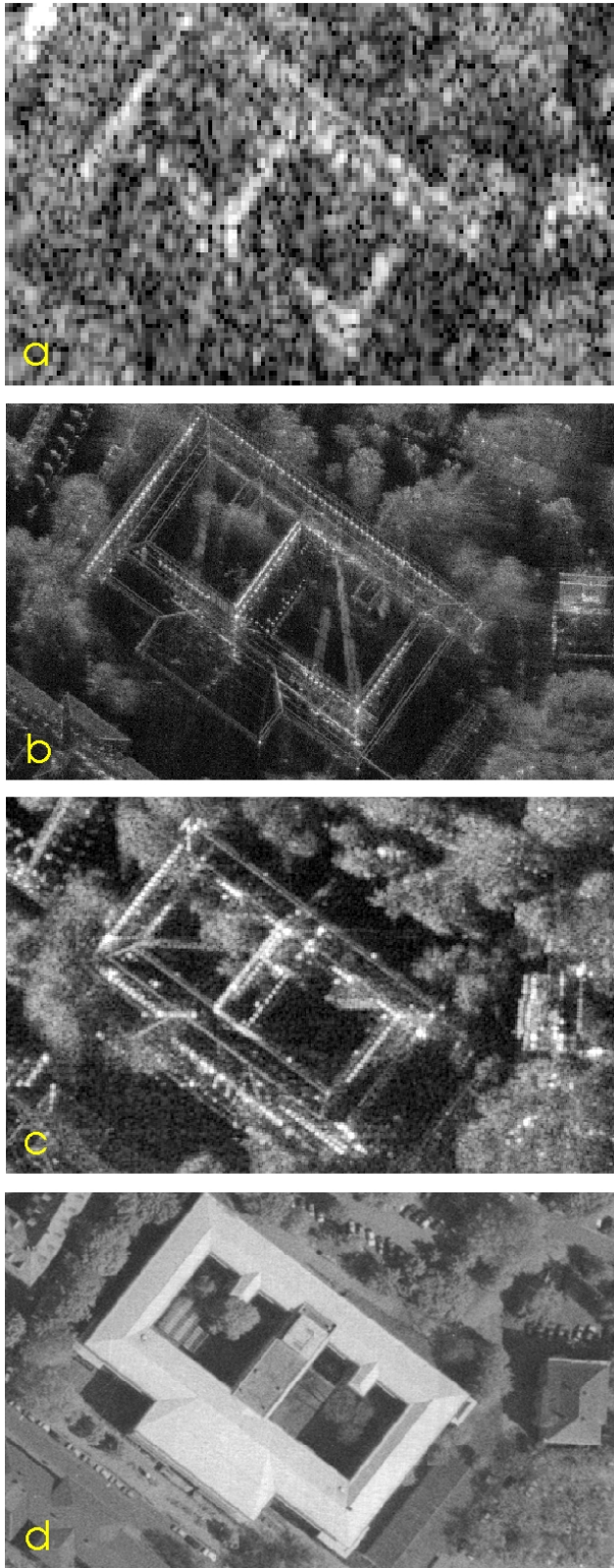
Fig.1 a) AER-II image with one meter resolution (range top-down, b) PAMIR image with resolution better than 20 cm (sliding spotlight mode, range top-down), c) PAMIR image with about 40 cm resolution (illumination from left), d) orthophoto (30cm)

Comparing the two SAR images 1a and 1b taken from the same aspect with different resolution, obviously in particular buildings look very different. Only a small number of scattering events occur and superimpose inside the small resolution cell of high-resolution SAR. Hence, much more building features like edges and point structures become visible, which were averaged with their surrounding background in SAR data of coarser resolution. This results as well in a larger dynamic range data especially in urban areas (about 70 dB for the PAMIR data). Due to the presence of only a limited number or in the extreme case only a single scattering event inside one resolution cell, SAR polarimetry [Guillaso et al., 2003] is expected to be of growing importance, e.g. to determine the orientation of structures and to overcome the layover problem.

A second PAMIR image is shown in Fig 1c. This time the illumination direction is from left to right. The image was focussed using strip map processing of a subset of the entire sliding mode data, resulting in approximately 40 cm resolution. Comparing the two PAMIR images some linear roof features and salient rows of point scatterers are visible in both images. Because of the orthogonal viewing directions on the other hand many complementing building features can be observed.

An orthophoto of the test scene is shown in Fig 1d. The PAMIR images and the aerial photo have about the same spatial resolution. Many features of the urban objects (buildings and vehicles) present in the scene can be observed in both frequency domains, but there are features, which appear in the SAR imagery but not in the aerial image and vice versa. Hence, a fusion of these complementing information sources for the analysis of urban structures seems to be fruitful [Tupin and Roux, 2004]. Furthermore, new opportunities for building recognition from SAR data arise from the high level of detail.

3. FUSION WITH GIS DATA

The interpretation of SAR imagery in dense urban scenes without supporting context information is a difficult task even for experts. However, context information is usually not available for all areas at the same level. The benefit from integrating GIS data in the analysis will be discussed for different levels of available data in the GIS: 2D maps, prismatic and polyhedral 3D city models.

3.1 2D map data

In the simplest case the availability of vector maps is assumed. In Fig. 2a and 2b the PAMIR images are shown in ground range projection (transformation from the slant range on a plane with given height h_g). The imagery was rectified using features on the ground that could be matched with their counterparts in the map and the orthophoto. The used tie points lie outside the shown part of the scene. The matching of tie points is a difficult task in built-up areas, because of occlusion and layover usually interfering large portions of the data.

Layers of building footprints (yellow) and roads (red) are superimposed on the SAR images. Due to the layover phenomenon, a shift towards the sensor position occurs between the locations of building footprints and the mapped building structures (mainly the roof) in the SAR data. Hence, layover areas can be clearly identified in this manner. They should be treated carefully in the further image analysis or even excluded from the interpretation. A road layer is often useful for the discrimination of roads from cast shadow of buildings. However, in this example the roads are not visible due to the presence of large deciduous trees.

3.2 Prismatic 3D city model

If elevation information is available, a different fusion approach is advantageous: the projection of the GIS data into the slant geometry according to the acquisition parameters of the SAR data. Fig. 2c shows in yellow the transformed roof eaves contours from a prismatic 3D city model superimposed on the slant range image. The location of the projected roof outlines is now correct. In addition the building footprints (red) have been projected in the same manner. Comparing the red and the yellow polygons in Fig 2c the layover region becomes more obvious: the area of the shift between the two projections contains the superimposed signal from the roof, the facade, and the ground in front. This shift visualizes also the geocoding error using a digital terrain model (DTM).

3.3 3D city model

The appearance of buildings in high-resolution SAR data is governed by large extent from roof structures. Those are represented in a polyhedral 3D city model. Figure 2d shows the edges of the roof structures of such a model superimposed on the SAR image, using the same transformation than before. Compared to the prismatic model, the cause of many additional linear features in the SAR data becomes now evident. The projected ridges and edges of the modelled roof patches coincide with their counterparts in the SAR data. In the case of imperfect geocoding a fine adjustment can be carried out by matching the transformed building model lines and segmented linear structures in the SAR image, such as those shown in Fig 3a. Additionally, polyhedral 3D city models can be used as reference data for the simulation of multipath signal propagation [Soergel et al., 2004]. However, many of the building features visible in the SAR image are not modelled in the 3D reference. Still, the detection of changes of urban structure using SAR seems to be a realistic option for the future. Additionally, existing 3D models could even be supplemented by integration of features provided in high-resolution SAR data.

4. RADARGRAMMETRIC ANALYSIS USING A PRODUCTION SYSTEM

Traditionally the recognition of the detailed geometric structure of urban areas from remote sensing data was restricted to aerial imagery and LIDAR. Such approaches in general exploit knowledge about frequently observed features of man-made objects such as straight edges, right angles, symmetries and regular or parallel alignment of object groups [Stilla and Jurkiewicz, 1999]. Until now, building recognition from SAR suffered mainly from the coarse level of detail of building features in the data [Soergel et al., 2003b]. As discussed before, in high-resolution SAR data many of such features became visible, which can now be incorporated into the analysis. Hence, it seems to be worthwhile to adapt existing methods e.g. for building recognition to SAR data. This will be sure a research topic for the next future when more of such data become available. Here, the potential of such an analysis is demonstrated by the radargrammetric determination of the height of a building based on the matching of salient angle structures of the roof. While the correlation or matching of low-level image structure is pointless due to different illumination, construction of correspondence between higher-level potential building structures makes sense. Furthermore, symmetry axes of buildings are derived. The assembly of more complex objects starting from primitives and the matching process are carried
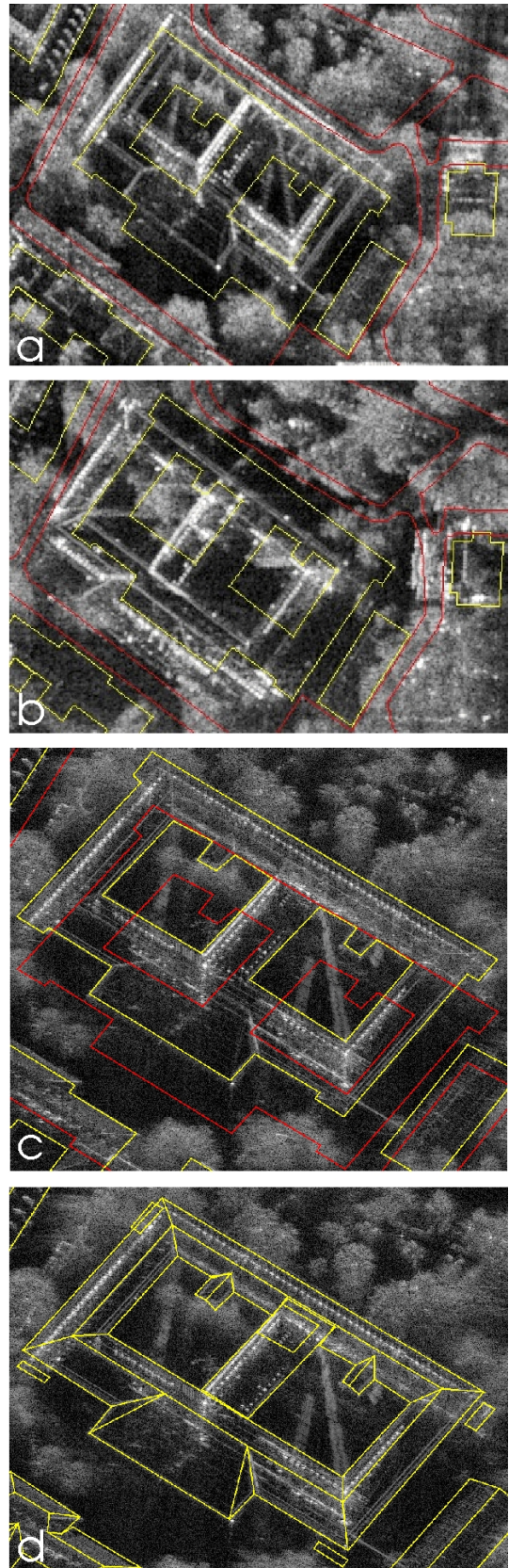

Fig.2 SAR images superimposed with building footprints (yellow) and roads (red): illumination from top a) and left b); c) projection of the building footprints (red) and the roof eave structures into the SAR geometry; d) like c) using the polyhedral 3D city model.

out by a production system. The production net [Stilla et al., 1996] shown in Fig 3 illustrates the workflow.
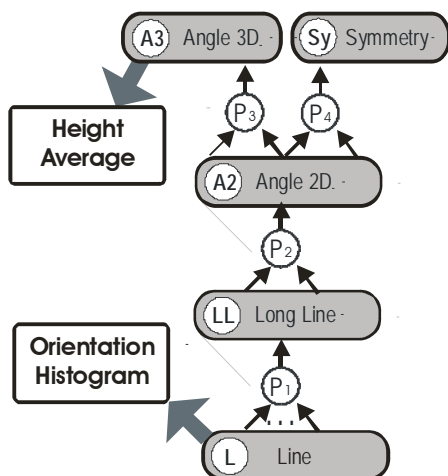

Fig. 3 Production net of the system.

4.1 Preprocessing

Because only a very limited number of high-resolution SAR data sets are available up to now, no adapted segmentation methods for such imagery are established yet. Instead standard tools were used for the investigations presented in the following. First, in a pre-processing step cropping of small numbers of very strong scatterers and choosing the 40dB of the signal starting from this threshold prune the large dynamic range of the data. Then the signal is mapped to byte format by non-linear operations. Finally, the images are first projected onto ground range and then coregistered.

4.2 Feature extraction and production system

Primitive line objects L are derived using the squared averaged gradient filter [Foerstner 1994]. Pixels where the first eigenvalue of this 2x2-Matrix is much bigger than the second one indicate the presence of either an edge or a line at that location. For this example 19.5% of the pixels of the two images have this property. Thus a set of over 100 000 objects L is inserted into the system.

From this set of objects L long line objects LL are built by production P_1. Small gaps between neighboured collinear primitives L are bridged in this step. This production first constructs only small prolongations of only several pixels length. But these lead to larger search regions, so that with increasing processing time longer objects LL are constructed that may well be several hundred pixels long. The next step is the assembly of 2D angle objects $A2$ from adjacent non-collinear objects LL with production P_2.

In the search run documented here some 12 500 objects $A2$ have been constructed from the primitives that describe the images content sufficiently well after 100 000 search cycles. These are displayed in Fig. 4a as red or green structures depending on the image in which they were found. For better interpretation the building layer from the map is shown as well. The productions P_3 and P_4 used for the feature matching and the search for building symmetries are discussed in the following paragraphs.
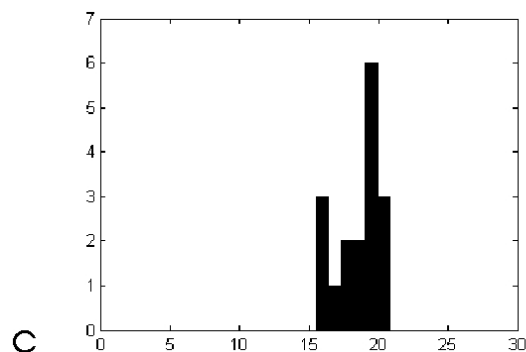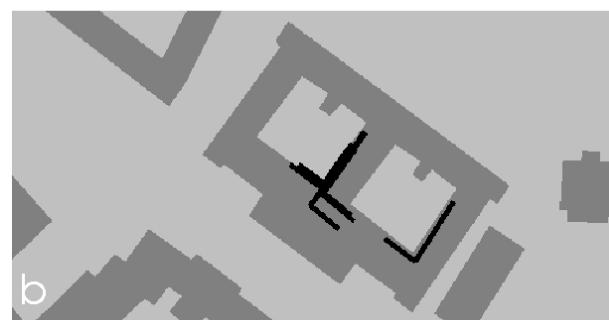

Fig.4 a) angle objects A2 after 100000 cycles b) 17 3D angle objects $A3$, c) height histogram of objects $A3$.

4.3 Feature matching

The situation after the coarse coregistration is illustrated in Fig 2a and 2b. Due to the orthogonal illumination, the layover shift is orthogonal, too, which becomes clear by comparing the building footprint with the images. The layover shift l_s of an elevated object depends on its height h over the elevation of the ground range plane h_g and the off-nadir angle θ.

$$l_s = h \cdot \cot(\theta)$$

The orthogonal illuminations lead to a straightforward strategy for the search of corresponding structures coded in production P_3. By exploiting geometric constraints it is possible to decide

whether two objects *A2* in the different images may result from the same 3D structure. Assuming a certain height of an angle object $A2_L$ produced in the image illuminated from the left results in a shift to the right in the world coordinate system coinciding with the image lines. Analogous, objects $A2_T$ found in the image taken from the top move with rising height downwards along the image column. From matching objects $A2_L$ and $A2_T$ a 3D angle object *A3* is constructed. The constraint resembles that of an epipolar line (going 45° from lower right to upper left here). It is very restrictive, so that even after 10 000 search cycles with the 12 500 angle objects *A2* only 17 objects *A3* are constructed. Fig. 4b shows that all of them belong to the dominant building in the middle. Fig. 4c gives the histogram of the derived heights in meter. From this a building height of 16.6m is estimated, which is close to the truth. In fact, the eaves of the building are 16 m above ground and the elevation variation of the mayor roof patches of about 2 m is small.

4.4 Intermediate Control Decisions

The processing effort is concentrated on objects of interest using decisions based on the set of objects inferred so far. The control is capable of preferring objects according to specified attributes or of concentrating on certain sub-systems of the net. In this case an orientation histogram on the objects *L* gives clear hints on the major orientations of the buildings in the processed area. The main effort is on the first stage, where only productions P_1 and P_2 are active. Productions P_3 and P_4 only take about 10% each of the search cycles that are spend on the lower subnet. However, it is clear that at least some of the constructions with the lower net have to be finished before these higher parts can become active.

If production P_3 succeeds in a height estimate it is useful to shift all the objects *A2* according to this. Then production P_4 can construct common symmetry patterns regardless whether the parts stem from one image or the other. Figs. 5a and 5b compare the results of the same search effort with and without such corrections. The following section gives the result.

4.5 Detection of building symmetry axes

The symmetry constraint is a non-local constraint and thus fairly weak. Whether on the shifted or original base of angles, production P_4 will come up with some 1200 objects *Sy* after 10000 search cycles. These are assessed according to the degree of their symmetry. Then they are clustered according to their axis. Figs. 5a and 5b display the objects *A2* underlying the clusters of sufficient size and assessment (again using colour code for the image from which they come). Of the 55 objects *A2* remaining in the original version 39 result from structure of the dominant building and 16 are from arbitrary other structures. Compared to this, the shifting leads to 59 objects *A2* where 46 result from structures of the dominant building and 13 from arbitrary other structures. Moreover, the 46 correct objects as well as the two major symmetries of the building are now correctly located in the scene. Symmetry patterns from one image and from the other image are clustered into the same correct axis estimations.

4.6 Future work

In an upcoming measurement campaign in fall 2005 the PAMIR system will be capable for InSAR measurements. Based on such data the building recognition approach will be extended.
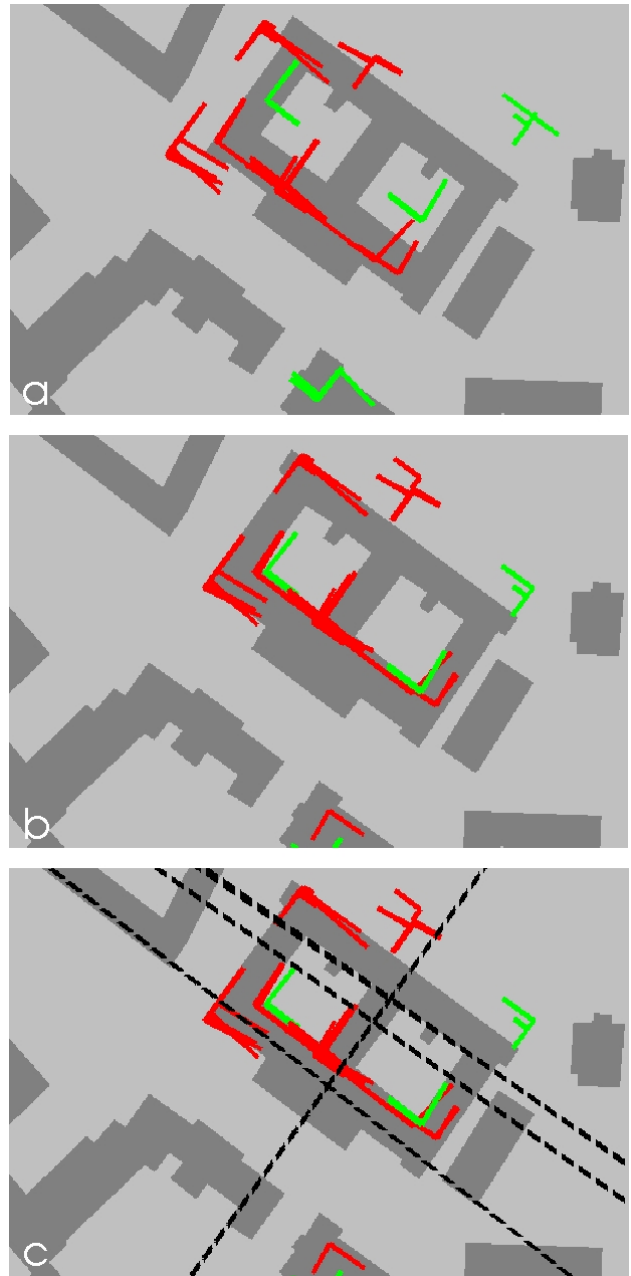

Fig.5 angle objects *A2* used for assembly of symmetry objects *Sy*: a) before, b) after shift, c) like b) plus the detected symmetry axes (black).

5. CONCLUSION

State-of-the-art high-resolution SAR sensors provide a detailed mapping of man-made objects, which could not be achieved by radar remote sensing only a few years ago. Structural image analysis approaches were up to now either tailored for extended targets or the extraction of rather coarse scene descriptions. In the new high-resolution data, a much finer level of detail of object features becomes visible. This supports efforts to use radargrammetric methods for the extraction of the structure of urban objects. Especially building recognition approaches from SAR data are expected to yield better results compared to the past, both in terms of accuracy and level of detail. First results based on multi-aspect SAR data presented here are

encouraging. Further improvements are expected to be possible from high-resolution InSAR data. The geocoding accuracy should match the resolution of the SAR data and therefore the height reference data must represent the buildings. Precise geocoding is a prerequisite e.g. for the fusion of multi-aspect SAR data or the fusion of SAR data with complementing data of different kind.

REFERENCES

Brenner, A. R., 2002. Distributed SAR processing in the time domain. Proc. of EUSAR, pp. 573-576.

Brenner, A. R. and Ender, J. H. G., 2002. First experimental results achieved with the new very wideband SAR system PAMIR. Proc. of EUSAR, pp. 81-86.

Dong, Y., Forster, B. and Ticehurst, C., 1997. Radar Backscatter Analysis for Urban Environments, Int. Journal of Remote Sensing, Vol. 18, No. 6, pp. 1351-1364.

Ender J.H.G., 1998. Experimental results achieved with the airborne multi-channel SAR system AER-II. Proc. EUSAR'98, pp. 315-318.

Ender, J. H. G. and Brenner, A. R, 2003. PAMIR - a wideband phased array SAR/MTI system. IEE Proceedings - Radar, Sonar, Navigation, vol. 150, no. 3, pp. 165-172.

Foerstner, W. 1994 A Framework for Low Level Feature Extraction. In: J.-O. Eklundh (ed). Computer Vision – ECCV 94, Vol. II, B1, pp. 383-394.

Gamba, P., Houshmand, B., Saccani, M., 2000. Detection and extraction of buildings from interferometric SAR data, IEEE Transactions on Geoscience and Remote Sensing, Vol. 38, No. 1, Part 2, pp. 611 –617.

Gouinaud, C., Tupin, F., and Maître, H., 1996. Potential and use of radar images for characterization and detection of urban areas. Proc. of IGARSS, 1996, pp. 474-476.

Guillaso, S., Ferro-Famil, L., Reigber, A., Pottier, E., 2003 Urban Area Analysis Based on ES-PRIT/MUSIC Methods using Polarimetric Interferometric SAR, Proc. Urban, Berlin, pp. 77-81.

Kakumoto, S., Hatayama, M., Kameda, H., Taniguchi, T., 1997. Development of disaster management spatial information system. Proc. GIS'97 Conf., pp. 595-598.

Leberl, F., 1990. Radargrammetric Image Processing. Artech House, Boston.

Lee, J. S. and Jurkevich, I., 1989. Segmentation of SAR images. In: IEEE Transactions on Geoscience and Remote Sensing, Vol. 27, p. 674-680.

Michaelsen, E., Soergel, U., and Thoennessen, U., 2004. Perceptual Grouping in Automatic Detection of Man-Made Structure in high-resolution SAR-Data. Workshop on Pattern Recognition in Remote Sensing, 2004, CDROM.

Roth, A., 2003. TerraSAR-X: A new perspective for scientific use of high resolution spaceborne SAR data, 2nd GRSS/ISPRS Joint Workshop on Remote Sensing and Data Fusion over Urban Areas, URBAN 2003, pp. 22-23.

Schreier, G., 1993. Geometrical properties of SAR images. In G. Schreier (ed.), SAR geocoding: Data and Systems: pp. 103-134. Karlsruhe: Wichmann.

Shinozuka, M., Ghanem, R., Houshmand, B., Mansuri, B. , 2000. Damage Detection in Urban Areas by SAR Imagery, Journal of Engineering Mechanics, Vol. 126, No. 7, pp. 769-777.

Simonetto, E., Oriot, H., Garello, R., 2003. Radargrammetric Processing for 3-D Building Extraction from High-Resolution Airborne SAR Data. IEEE Int. Geoscience and Remote Sensing Symosium, IGARSS 2003, Toulouse, Vol. 3, pp. 2002-2004.

Soergel, U., Michaelsen, E., Thoennessen, U., Stilla, U. 2005 Opportunities of Urban Analysis from High-Resolution SAR Data. ISPRS Hannover Workshop 2005: High-Resolution Earth Imaging for Geospatial Information, in print.

Soergel, U., Schulz, K., Thoennessen, U., Stilla, U., 2003a. Event-driven SAR Data Acquisition in Urban Areas Using GIS, GeoBIT/GIS Journal for Spatial Information and Decision Making, Huethig Verlag, Heidelberg, Vol. 12, 2003, pp. 32-37.

Soergel, U., Thoennessen, U., Stilla, U., 2003b. Reconstruction of Buildings from Interferometric SAR Data of built-up Areas, in: Ebner H, Heipke C, Mayer H, Pakzad K (eds) Photogrammetric Image Analysis PIA. International Archives of Photogrammetry and Remote Sensing. Vol. 34, Part 3/W8, pp. 59-64.

Soergel, U., Thoennessen, U., Stilla, U., 2004. SAR Data Acquisition for Event-driven Mapping of Urban Areas Using GIS. In: International Archives of Photogrammetry and Remote Sensing. Vol. 35, pp. 500-505.

Stilla, U., Jurkiewicz, K., 1999. Reconstruction of building models from maps and laser altimeter data. In: Agouris, P., Stefanidis, A. (eds.), Integrated spatial databases: Digital images and GIS: 34-46. Berlin: Springer.

Stilla, U., Michaelsen, E,. Lütjen, K. 1996. Automatic Extraction of Buildings from Aerial Images, in: F. Leberl, R. Kalliany, M. Gruber (eds.), Mapping Buildings, Roads and other Man-made Structures from Images, IAPR-TC7, Wien, Oldenburg, pp. 229-244.

Stilla, U., Michaelsen, E., Soergel, U., Hinz, S., Ender, H. J. G., 2004. Airborne Monitoring of Vehicle Activity in Urban Areas. International Archives of Photogrammetry and Remote Sensing. Vol. 35, Part B3, pp. 973-979.

Takeuchi, S., Suga, Y., Yonezawa, C., Chen, CH., 2000. Detection of urban disaster using InSAR - a case study for the 1999 great Taiwan earthquake. Proc. IGARSS, CD ROM.

Tupin, F., Roux, M., 2004. 3D Information extraction by structural matching of SAR and optical features. In: International Archives of Photogrammetry and Remote Sensing. Vol. 35.